

Continuation Load Flow Considering Discontinuous Behaviors of Distribution Grids

Luan F. S. Colombari, Roman Kuiava, *Member, IEEE*, Vedran Peric, *Member, IEEE*, and Rodrigo A. Ramos, *Senior Member, IEEE*

Abstract—The reduction in bus voltage magnitudes as the load demand grows may lead to sudden disconnection of loads and/or distributed generation units, in distribution grids, caused by undervoltage protection schemes. As proposed in this paper, this discontinuous behaviour of distribution grids can be modeled as a sudden load variation in traditional static Voltage Stability Assessment methods, such as the continuation power flow (CPFLOW). A discussion on the impacts of these discontinuities on the equilibrium diagram of the system is presented in this paper, as well as a set of numerical simulations showing that the traditional CPFLOW algorithm presents convergence problems caused by the discontinuities under analysis. From this perspective, this paper proposes an algorithm based on novel predictor/corrector and identification schemes, which are capable of successively calculating the discontinuities that exist in the equilibrium loci of the system under analysis, as well as the Maximum Loadability Point and the type of bifurcation. A simplified modeling approach that eliminates the need for a complex (and computationally expensive), detailed description of distribution grids is also elaborated and incorporated into the proposed algorithm. The simulated examples show that the proposed algorithm adequately handles the problem, yielding more accurate results than the traditional CPFLOW algorithm.

Index Terms—Voltage stability, load modeling, continuation power flow, predictor/corrector method.

I. INTRODUCTION

POWER systems are nowadays operated closer to their limits in an overall sense, which makes them more prone to voltage stability problems. One example of voltage instability was seen in Brazil in 2009, when the three transmission lines that deliver power from the Itaipu power plant to the bulk power grid were disconnected. This disturbance caused voltage sags in the state of Sao Paulo, which resulted in disconnection of the HVDC link between Brazil and Paraguay [1]. Problems like this motivated this research, with the aim of developing more robust and accurate voltage stability assessment algorithms, that can upgrade or even replace the traditional voltage stability assessment tools [2].

Traditional Voltage Stability Assessment (VSA) methods typically rely on algorithms that assume a continuous behaviour of the load [3], which is an assumption that may

not hold in practice, taking into account several particular characteristics of current power systems operation, such as the presence of undervoltage load shedding (ULS), distributed generation (DG) undervoltage protection, and modern demand side management schemes [4]. In the case of DG, these small generators may exhibit discontinuous behaviours (due to protection actuation) during disturbed operational regimes, in order to comply with the grid codes. Also, typical load shedding and demand side management schemes clearly produce discontinuous behaviours of the loads in distribution grids. Several authors have tried to address this issue as reported in [5] and [6] where the mandatory disconnection of DG was considered during dynamic simulations. In [5], it was demonstrated that inadvertent undervoltage trip of a DG unit may cause instability in bulk power systems. In [6], a transmission system Maximum Loadability Point (MLP) was estimated from small successive increments in its load. This study concluded that mandatory disconnection of DGs units may cause a significant reduction in the Voltage Stability Margin (VSM) of the system. Both studies are based on dynamic voltage stability analyses, which provide accurate results but are often too computationally expensive for control center applications.

A practical alternative to dynamic analysis comprises static techniques employing the power flow problem formulation and the estimation of equilibrium diagrams or PV curves of the system [7]–[9]. A reliable technique to trace equilibrium diagrams of power systems and to estimate their MLPs is the Continuation Power Flow (CPFLOW) method [2], [7]. However, traditional algorithms based on CPFLOW suffer from several convergence issues in cases where the system exhibits discontinuous behaviours. Examples of equipments with discontinuous behaviour are switchable shunt capacitors and excitation limiters of generators [10]. These devices are responsible for sudden structural (parametric) changes in the power system model which, in turn, causes discontinuities in its equilibrium diagram. There have been several attempts to analyze voltage stability in the presence of discontinuities. For example, in [10]–[12], generator reactive limits (Q-limits) as well as switching capacitors were considered. However, none of these contributions treat other types of system discontinuities such as ULS schemes or mandatory DG disconnections.

This paper attempts to fill this gap in static VSA methods by taking into account these discontinuous behaviours of distribution grids. First, the paper proposes a simple but efficient method to model discontinuities in the distribution grids, which eliminates the need for a detailed representation of these

Luan F. S. Colombari is with the Brazilian Navy, Rio de Janeiro, Brazil, e-mail: colombari@marinha.mil.br.

Roman Kuiava is with the Department of Electrical Engineering, Federal University of Parana (UFPR), Curitiba, Brazil, e-mail: kuiava@eletrica.ufpr.br.

Vedran Peric is with the General Electric (GE) Energy Consulting, Munich, Germany, e-mail: vedran.peric@ge.com.

Rodrigo A. Ramos is with the Department of Electrical Engineering, University of Sao Paulo (USP), Sao Carlos, Brazil, e-mail: rodrigo.ramos@ieee.org.

Manuscript received —; revised —.

grids. Then, the paper proposes an algorithm that incorporates novel predictor/corrector and identification schemes, which accounts for discontinuous behaviours of the system and then identifies the MLP and the type of bifurcation, which can be either a Saddle-Node Bifurcation (SNB) or a Structure Induced Bifurcation (SIB). In contrast to [10] where the step size is adaptively changed according to the results of the convergence monitor, the proposed method identifies the point of occurrence and the type of discontinuity and treats them accordingly.

The paper is organized as follows. Sections II and III provide the problem statement and proposed modeling of the discontinuities in the distribution grids, respectively. In Section IV a description of the proposed algorithm is given and the results obtained for the 118 bus IEEE test system are shown in Section V. Final conclusions are drawn in Section VI.

II. STATIC VSA FUNDAMENTALS AND THE CPFLOW

Let $P_L(\lambda)$ and $Q_L(\lambda)$ be, respectively, the vectors of active and reactive power demand in the system buses, parameterized by the load parameter λ . Considering $\lambda = 1$ as the current operating point (or the base case demand) of the system, the load growth parametrization can be written as

$$P_L(\lambda) = P_{L0} + (\lambda - 1)K_P P_{L0}, \quad (1)$$

$$Q_L(\lambda) = Q_{L0} + (\lambda - 1)K_Q Q_{L0}, \quad (2)$$

where P_{L0} and Q_{L0} are the active and reactive power demands, respectively, associated with the base case load of the system. K_P and K_Q are vectors that determine the growth proportion of the load in each bus.

The power flow equations with the load growth parametrization (1)-(2) can be written in the compact form:

$$0 = F(x) + \lambda b, \quad (3)$$

where b is the vector of the load growth direction, which is composed by K_P and K_Q . Also, x is the vector with the power system state variables (that is, bus voltage angles and magnitudes). $F(x)$ is a vector with nonlinear functions of the state variables.

Varying the load parameter λ and solving the resulting power flow equations (3), the equilibrium diagram (i.e., the PV curve) of the system can be drawn according to the load growth direction determined by b . The nose of the PV curve represents the MLP and it is a bifurcation point of the system. The closer system operates to the MLP, the more likely it is to be subject to voltage instability. In this context, the Voltage Stability Margin (VSM) is defined as the distance from the power system current loading to its maximum value [8].

The CPFLOW is regarded as an efficient and precise method to estimate the MLP and obtain PV curves, specifically designed to deal with the ill-conditioning of the Jacobian matrix close to the MLP. It basically consists of three steps: parametrization, prediction and correction. These three steps are briefly discussed below.

Parametrization: during the execution of the CPFLOW, the scalar λ is also regarded as an unknown variable, which makes the system (3) underdetermined, once the number of

variables exceeds the number of non-linear equations by one. The parametrization procedure consists in including another equation to this problem, where a selected state becomes fixed (namely, the continuation parameter), so the parameter λ can be found together with the other power system states by a Newton-Raphson method, for example. An adequate choice of the continuation parameter near the MLP can avoid the problem of an ill-conditioned Jacobian of the power flow equations in this region. This continuation parameter can be a bus voltage magnitude or angle, or even the load parameter λ [13], but λ is typically not used near the MLP.

Prediction: the purpose of the prediction stage is to find an approximate solution that is close to the next power flow solution defined by the next step in the continuation parameter. The most commonly employed predictors are based on linear approximations [7].

Correction: after the prediction stage finds an approximation to an equilibrium point of the system, the correction stage is designed find this equilibrium point by solving the power flow equations (3) with the desired accuracy. The starting point of the numeric procedure adopted to solve (3) (typically by a Newton-Raphson method) is the approximation obtained in the prediction stage. Since this result is usually close to the actual power flow solution, the Newton-Raphson method is expected to converge in a few iterations [7], [12], [13].

A. The Evolution of the CPFLOW to Deal With Discontinuities

The prediction stage employs curve fitting approximations and it is not able to consider possible discontinuities that may be present in power system equilibrium diagrams. It is the corrector that is responsible to handle them. This is achieved within the Newton-Raphson numeric procedure, with conditions that guarantee proper description of the system behaviour. As a result of that, when a discontinuity occurs, the predictor provides a less accurate approximation, thus requiring more iterations of the correction stage [7].

For this reason, several studies deal with the computational efficiency of the CPFLOW. Alongside with time performance, many researchers study the negative effect of Q-limits on the MLP [10]–[12]. A great interest lies on how to identify these points especially when they cause a bifurcation and how these discontinuities influence the CPFLOW execution. For example, in [14] the authors proposed the repetition of continuation steps with reduced step sizes when the system is apparently close to a bifurcation caused by a Q-limit. With this method it is possible to identify the bifurcation point and the generator that caused it. However, for this purpose it requires a few extra continuation steps. [11] employed an arc-length parametrization and proposed that the continuation step should be selected with the purpose of predicting the next generator that will reach its Q-limit.

Paper [12] enhanced the work of [15] by proposing a parametrization that is based on generator Q-limits. After the prediction and correction, the method results in the next power flow solution where one generator reaches its reactive limit. With this method, all Q-limits that happen before the MLP are calculated. The number of continuation steps required is equal

to the number of such constraints, which can be significantly lower than the the number of steps in a standard CPFLOW. The main contribution of this paper is that the continuation step is automatically selected to be equal to a continuous portion of the PV curve, *i.e.*, the arc between two discontinuities.

The next section discusses the proposed distribution system model that incorporates discontinuous behaviour due to ULS schemes and mandatory disconnection of DG units. This approach was already presented by the authors in [16], but here the model is generalized to incorporate both types of discontinuities.

III. PROPOSED EQUIVALENT DISTRIBUTION SYSTEM MODEL TO ACCOUNT FOR OPERATING DISCONTINUITIES

Two types of discontinuities in the operation of distribution grids are considered in this paper: decentralized ULS and mandatory disconnection of DG units due to undervoltage protection actuation. First, in order to predict the mandatory disconnection of DGs, it is necessary to estimate the voltage drop of the feeder from the substation bus associated with the unit to its Point of Common Coupling (PCC). The voltage drop along the feeder and, consequently, the DG undervoltage protection actuation depends on the power injected by the unit, the feeder impedance parameters, and the system loading level. In general, this information is not available to transmission system utilities and, therefore, simplifying assumptions are necessary. Here, three assumptions are made based on general characteristics of distribution systems: (i) substations are equipped with an On-load Tap Changing transformer (OLTC) operating at its maximum control limit before any DG disconnection takes place; (ii) DG units supply only active power to the distribution system and this injection is independent of the voltage magnitude at the PCC; and (iii) DG units connected to a given substation can be divided into three groups according to the voltage drop from the substation to their PCC. Group 1 is close to the substation and is not subject to any voltage drop. Group 2 is located at the middle of the feeder and the voltage drop is assumed to be 0.015 pu. Finally, Group 3 is located at the end of the feeder with a voltage drop is assumed to be 0.030 pu.

Assumption (i) is realistic and based on the common practice of employing a transformer capable to change/control its tap under load in distribution substations. It is reasonable to assume that the control margin of this OLTC has reached its regulation limit before there is pick-up of any DG undervoltage protection. The maximum tap is considered to have been reached when the voltage ratio is 10% above its nominal value. The second assumption is related to the common use of unity power factor control for distributed generators [17], [18]. The third assumption is obviously an approximation, but the alternative to it would depend on information regarding distribution systems that is usually unavailable to transmission operators. For this reason, including detailed models of distribution feeders would only replace the assumed voltage drops by other unknown parameters and variables of these circuits.

The other discontinuity considered in this paper is caused by ULS schemes, which are designed for very unlikely scenarios

that could be cumbersome to system operation and even cause voltage collapse [19]–[22]. To meet its goals, ULS schemes must be carefully designed. Two approaches can be distinguished for this purpose: the decentralized and the centralized schemes. The centralized one is based on the status of the complete power system as measured by the control center, from where, if necessary, the location and amount of load to be shed is determined and carried out through communication networks. The local scheme is simpler and based on local measurements of bus voltages that can automatically disconnect their associated loads [23]. As a result of them, load is shed if particular bus voltage magnitudes drop below some threshold for a given time interval [19], [24]. In this paper, a decentralized ULS scheme is analyzed where different levels of load can be shed. These loads can be located anywhere in the feeder.

The distribution system model resulting from the three assumptions made for the mandatory disconnection of DG units and the for decentralized scheme for ULS is indicated in Fig. 1. The three groups of DG units are individually paired with a distinct feeder voltage drop. V_t and V_s are the voltage magnitudes at the high and low voltage sides of the OLTC, respectively. The other buses correspond to the ones where the voltage drop with respect to V_s is equal to 0.015 pu and 0.030 pu, respectively. DG group i will have its associated units tripped due to their PCC undervoltage protection when (4) is satisfied.

$$V_t \leq (V_{drop_i} + V_{prot})/1.1, \quad i = 1, 2, 3, \quad (4)$$

where V_{prot} is the undervoltage pick-up value of the DG PCC protection and V_{drop_i} is the feeder voltage drop of DG group i . The denominator is related to the OLTC maximum control margin.

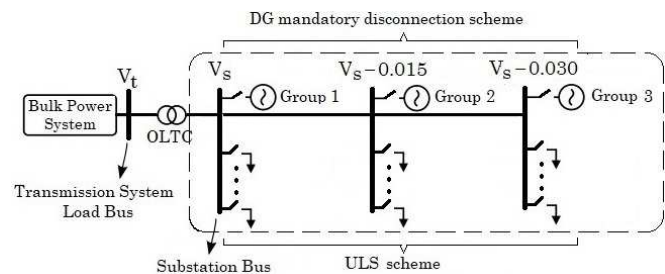


Fig. 1: Proposed distribution system model.

In the context of the CPFLOW, the discontinuities in the operation of distribution grids (due to mandatory disconnection of DG units and ULS schemes) can be modeled as sudden changes in the equivalent load of the respective substation. Let us consider m combinations among the operational state (switched on or off) of the groups of DG units and the loads tripped by the ULS scheme. Each combination leads to a specific equivalent load of the distribution grid connected to the bus i at the base case demand, *i.e.* $P_{L0_i}^j$ and $Q_{L0_i}^j$, $j = 1, \dots, M$. This corresponds to M different levels of load growth parametrization for bus i :

$$P_{L_i}^j(\lambda) = P_{L0_i}^j + (\lambda - 1)K_{P_i}P_{L0_i}^j \quad (5)$$

$$Q_{L_i}^j(\lambda) = Q_{L0_i}^j + (\lambda - 1)K_{Q_i}Q_{L0_i}^j, \quad j = 1, \dots, M \quad (6)$$

During the execution of the CPFLOW, depending on the operational state of the groups of DG units and loads for a specific load parameter λ , the load growth parametrization will jump among these M different levels, causing discontinuities in the resulting PV curve. Notice that for the same value of λ there can be different corresponding values of active and reactive powers for each $j = 1, \dots, M$. Therefore, any jump in the load growth parametrization level can be viewed as a sudden change in the load of a specific bus.

A. An illustrative example

In order to illustrate the fact that the sudden connection/disconnection of DG units and loads will cause discontinuities in the resulting PV curve, consider as an illustrative example the simplified power system shown in Fig. 2(a). This system has a large generator (G1), a transmission line between buses 2 and 3 and a distribution grid (bus 4). This distribution grid has some DG units and an ULS scheme, as described by Fig. 1. In addition, let us assume that all the DG units of bus 4 belong to group 1, in accordance to Fig. 1. Hence, the DG groups 2 and 3 are not considered in this illustrative example. The group of DG units and a part of the load can be disconnected (due to the ULS scheme) if the voltage magnitude at bus 4 reaches a value equal to V_{off1} and V_{off2} , respectively.

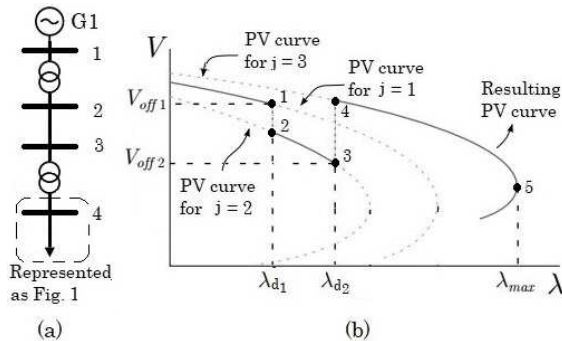


Fig. 2: (a) An example of power system for static VSA analysis; (b) Resulting PV curve due to discontinuous operation of the distribution grid.

Then, there are 3 different load levels ($M = 3$), in accordance to (5)-(6). For $j = 1$, the group of DG units and the entire load at bus 4 are switched on; $j = 2$ corresponds to the case where the group of DG units is switched off and the entire load at bus 4 is on; and for $j = 3$, the group of DG units and a part of the load at bus 4 are switched off.

For each possible load growth parametrization level, the PV curve of bus 4 can be traced using the traditional CPFLOW algorithm, as indicated with dashed curves in Fig. 2(b). The resulting PV curve of the system, which considers the disconnection of the group of DG units when the local voltage reached V_{off1} (points 1 and 2) and when part of the load is shed in V_{off2} (points 3 and 4) is shown in this same figure, as the solid curve. The MLP is given by (λ_{max}). It is important to point out that the sudden changes in the power demand for λ_{d1} and λ_{d2} are supplied by G1. Observe that the power system equilibrium diagram exhibits a jump between PV curves, which characterizes state discontinuities.

IV. PROPOSED ALGORITHM

The proposed algorithm is divided into four stages as follows: (i) Discontinuity prediction; (ii) Correction stage I - pre-discontinuity; (iii) Correction stage II - post-discontinuity and; (iv) Identification of MLP and bifurcation type. The process involving these four stages is schematically described in the flowchart of Fig. 3. The output data of the algorithm comprises the sequence of discontinuities to which the power system equilibrium diagram is subject to (as well as the estimation of the MLP and VSM). Each part of the flowchart will be described separately in the following subsections.

A. Discontinuity Prediction

The goal of this stage is to anticipate what is the next discontinuity that will happen as the load grows and at which system state it will take place. For that, a linear approximation based on the tangent vector to the equilibrium diagram is employed. This tangent vector at a known power flow solution (x_1, λ_1) is calculated from

$$0 = \frac{dF(x)}{dx} \Delta x + b \Delta \lambda \quad (7)$$

where Δx and $\Delta \lambda$ are deviations of the system state x and the load parameter λ from the actual values x_1 and λ_1 , respectively. They correspond to the tangent vector components. To solve this linear system, the Jacobian is evaluated at a known power flow solution and an arbitrary value is assigned to $\Delta \lambda$ or to an element of Δx . Afterwards, for each bus that contains a distribution grid with undervoltage protection devices capable to switch off DGs and/or loads, the linear distance from the known equilibrium to the point where the protection trips is estimated by

$$\sigma_i = (V_i - V_i^{pick}) / \Delta V_i \quad (8)$$

where V_i^{pick} is the undervoltage pick-up value that would switch off DG units or loads in bus i and V_i is the actual bus voltage magnitude at the known power flow solution x_1 . ΔV_i is the component of the tangent vector Δx that corresponds to the bus voltage under analysis. The calculated value σ_i is an estimate of how close bus i is from triggering its undervoltage protection. Therefore, the next discontinuity in the PV curve will be the one associated with the smallest value of σ_i .

The bus that is associated with the smallest σ_i (σ for short) will be used in the correction stages, where it will be referred to as the pivot bus and indicated by letter p . After that, the system states can be estimated from the tangent vector by:

$$x'_2 = x_1 + \sigma \Delta x, \quad \lambda'_2 = \lambda_1 + \sigma \Delta \lambda \quad (9)$$

Therefore, λ'_2 is the prediction of the next load parameter value at which a discontinuity in the PV curve will occur. Fig. 4(a) shows again the PV curve of Fig. 2(b), but illustrating the prediction step with the initial power flow solution (λ_1, x_1), the continuation step σ and the state estimation (λ'_2, x'_2).

B. Correction Stage I - Pre-discontinuity

The goal of this stage is to calculate the power flow solutions within the desired accuracy to find the power system

equilibrium point right before the predicted discontinuity takes place (in Fig. 2(b), for example, right before λ_{d1} or λ_{d2}). To achieve that, the power flow problem formulation is augmented with the parametric equation that sets the pivot bus voltage magnitude equal to its undervoltage protection setting.

$$V_p - V_p^{pick} = 0 \quad (10)$$

The augmented set of equations is solved with the Newton-Raphson method, resulting in the system states together with the load parameter, that is, (λ_2, x_2) (see Fig. 4(b), point 1 of the curve in the middle). The starting point of the numerical method employed here is the power system state (λ'_2, x'_2) predicted with (9).

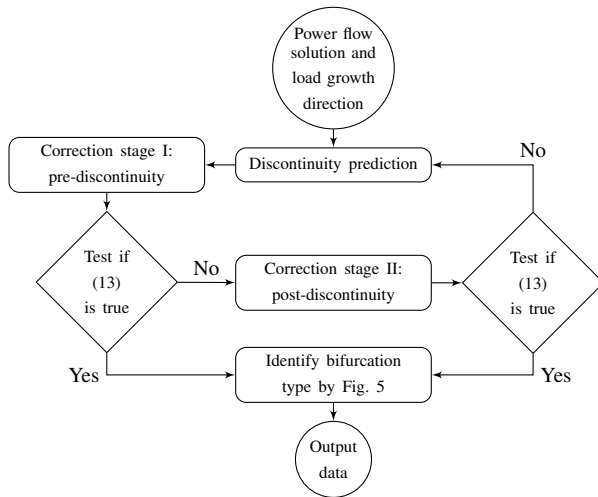


Fig. 3: Flowchart of the proposed algorithm.

C. Correction Stage II - Post-discontinuity

A second corrector is necessary to find the power flow solution right after the discontinuity takes place (in Fig. 4(a)-(b), for example, point 2 in the lower curve). Prior to this correction stage, it is not feasible to employ a predictor. This happens because it deals with the actual occurrence of the discontinuity, *i.e.*, a jump between two PV curves. In this situation, approximations based on curve fitting techniques are not expected to be accurate. The correction stage II employs the Newton-Raphson method to find the equilibrium point of the system right after the distribution grid discontinuity anticipated by the predictor. The initial guess for this numeric method will be the solution obtained from the correction stage I. In Corrector II, the parametric equation employed depends on whether the equivalent load of the substation bus is suddenly increased or reduced, as follows.

Sudden equivalent load reduction: As depicted in Fig.2(b), right after a discontinuity in the distribution grid, the parameter λ does not change, the discontinuity is observed in the system state. This fact can be well reproduced if λ is selected for the parametrization. This means that the power flow equations need to be solved simultaneously with the following equation:

$$\lambda - \lambda_2 = 0 \quad (11)$$

where λ_2 is the load parameter that was obtained from the corrector stage I. After executing the Newton-Raphson

method, the system equilibrium calculated will be (λ_3, x_3) . The parametric equation employed guarantees the load parameter before and after the sudden load variation will be the same, that is, $\lambda_3 = \lambda_2$. This characterizes correctly the nature of the discontinuity under analysis. In Fig. 4(a), for example, the point 2 given by (λ_2, x_3) in the lower curve is obtained after the application of the corrector stage II at point 1 (λ_2, x_2) in the upper curve.

Sudden equivalent load increase: After an increase in the equivalent load of the substation bus, like the one that would result from the disconnection of a DG group, a reduction in the VSM is expected. Therefore, employing λ for the parametrization may lead to convergence problems due to ill-conditioning of the Jacobian matrix, since the power system is getting closer to the bifurcation.

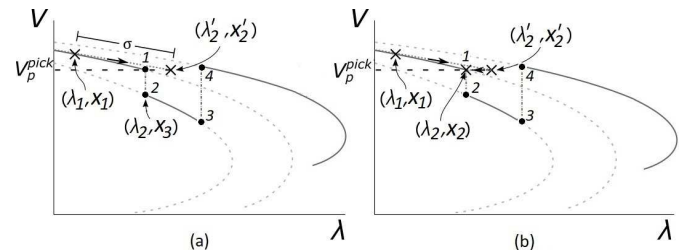


Fig. 4: Graphical representation of the predictor (a) and corrector I (b).

The pivot bus voltage magnitude used in the correction stage I is also employed in this case. This is described in (12), where $V_p(\lambda_2)$ is the voltage magnitude of the pivot bus at the solution of Corrector I.

$$V_p - V_p(\lambda_2) = 0 \quad (12)$$

The voltage $V_p(\lambda_2)$ is an element of the state vector x_2 and, due to the parametric equation employed in Corrector I (10), it is equal to V_p^{pick} .

D. Identifying the MLP and Bifurcation Type

The tangent vector (7) can be used to identify whether or not the MLP has been exceeded, that is, if a given power flow solution lies in the stable upper portion of the PV curve or in the unstable lower one [7]. Therefore, after every correction step, the tangent vector of the calculated equilibrium is used to assess if an unstable point was found. The power flow solution is an unstable equilibrium point if a load increase leads to an increase of voltage, which is determined by the following criterion:

$$\text{sign}(\Delta V_p) = \text{sign}(\Delta \lambda) \quad (13)$$

where $\Delta \lambda$ and ΔV_p are components of the tangent vector $(\Delta \lambda, \Delta x)$. When (13) is satisfied, the proposed method should stop solving the power flow equations and an algorithm should be employed to identify the bifurcation type to which the system was subject. Two conditional tests are employed to identify if the MLP is a SNB or a SIB one. These conditions are summed up in Fig. 5, where x_{sup} and x_{bel} are the last power flow solutions calculated that lie in the superior and inferior portion of the PV curve respectively. Also, x_{maj} is the power system state, among all power flow solutions calculated, that is associated with the highest value of the loading

parameter λ . In other words, this state is selected among the equilibrium points found with the proposed predictor/corrector scheme.

Condition I deals with the situation where one generation disconnection leads to instability. In this case, the last two power flow solutions found (x_{sup} and x_{bel}) are not the ones that correspond to the highest load level (x_{maj}). This happens because a previous sudden load variation (the one associated x_{maj}) was large enough to cause big voltage drops across the power system (to an extent that these voltage drops can lead to other discontinuities and even produce instability). In this situation x_{maj} is a SIB.

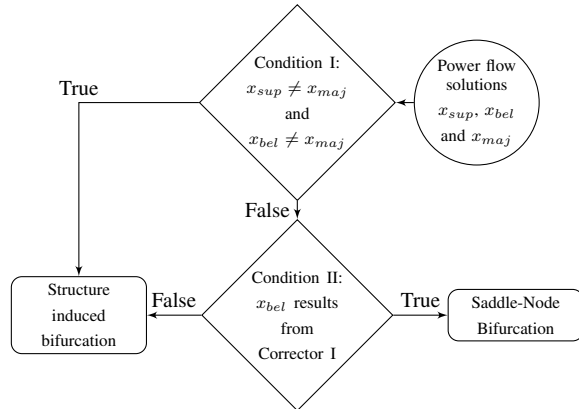


Fig. 5: Flowchart of the identification algorithm.

The meaning of Condition II depends on the unstable equilibrium (x_{bel}) being a result of Corrector I or II. If x_{bel} results from Corrector I, then the bifurcation happened between two discontinuities in a continuous arc of the PV curve. As a result of that, between these two solutions there is necessarily a SNB. In this case another method (such as the traditional CPFLOW, for example) should be employed to accurately find the MLP, since the algorithm described here only calculates equilibrium points related to sudden parametric variations. If Condition II is false, the solution lying in the lower portion of the PV curve results from Corrector II. In this situation, the discontinuity under analysis in this step is the cause of the unstable equilibrium found, characterizing a SIB. Fig. 6 illustrates a scenario when Condition II is satisfied and a SNB is identified.

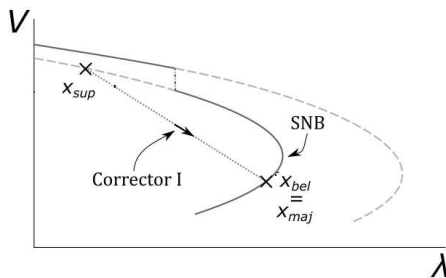


Fig. 6: Graphical representation of the identification of MLP and bifurcation type.

V. TESTS AND RESULTS

This section illustrates the application of the proposed algorithm described in the last section and compares it with

the traditional CPFLOW algorithm with local parametrization in terms of MLP estimation. The results were obtained for the IEEE 118 bus test system [25], [26]. This system has 118 buses, of which 53 are PV buses and 64 are PQ buses. Also, the system has 186 lines and a total active load equal to 3.668 GW.

A. Tests Considering Mandatory Disconnection of DG Units

This subsection addresses the effect of the DG undervoltage mandatory disconnection on the VSM and MLP of the previously mentioned test system. For that, a few simplifying considerations were made:

- The load growth was parametrized as described by (1)-(2) considering that K_P and K_Q are vectors with all elements equal to one. Also, to meet this load increase, generators are dispatched proportionally to their base case active power injection.
- DG units were included in every load bus according to the model in Fig. 1.
- Three levels of DG penetration were considered during the numerical studies: 10%, 20% and 30%. These levels represent the percentage of the load at each bus that is supplied by DG.
- For each load bus, the total DG power injection was equally divided between the three groups of the proposed distribution system model depicted in Fig. 1.
- All distributed generators have the same undervoltage protection settings at their PCC. Tests were made for the values of 0.95 pu and 0.85 pu.
- The algorithm described in this paper was implemented together with the method proposed by [12]. When combined, they can find the load levels associated to both generator reactive power limits and DG undervoltage disconnection.

Also, the power supplied by DG units at each load bus is available in [27]. The three DG penetration levels and the two undervoltage protection settings considered created several scenarios to study situations where the DG mandatory disconnection is critical to the system stability and situations where it is not relevant. All methods employed are considered to have converged if one unstable equilibrium is found. Only the scenarios corresponding to the DG undervoltage protection set at 0.95 pu will be shown. The other ones are available in [27].

For the three cases with the referred protection settings, the MLP and the VSM are indicated in Tables I and II, for the traditional CPFLOW and the proposed method respectively. These tables also present the absolute amount of DG that was disconnected in MW and the percentage of the total DG injection that was lost.

With exception of the base case, where the system is not subject to DG mandatory disconnection, the CPFLOW diverged for all considered scenarios, *i.e.*, no solution was found in the inferior portion of the PV curve. The MLP and VSM indicated in Table I are related to the last power flow solution found before divergence of the method. The continuation step-size employed to find these results was chosen after several

trial and error attempts to make the CPFLOW converge and the actual value selected was the one associated with the higher loading level of the last converged solution. In contrast, the proposed algorithm converged for these three cases. The VSM of both methods are similar, which indicates that the CPFLOW diverged close to the MLP.

TABLE I: Results obtained from the traditional CPFLOW.

DG penetration level	λ_{max}	VSM		DG Disconnection	
		(GW)	(%)	(MW)	(%)
0%	2.126	4.13	113	-	-
10%	2.111	4.07	111	69	19
20%	2.085	3.98	108	123	17
30%	2.072	3.93	107	201	18

TABLE II: Results obtained from the proposed algorithm.

DG penetration level	λ_{max}	VSM		DG Disconnection	
		(GW)	(%)	(MW)	(%)
10%	2.113	4.08	111	75	21
20%	2.093	4.01	109	170	23
30%	2.073	3.93	107	279	25

From the results of the proposed scheme, it is possible to state that the CPFLOW was not capable to trace the nose of the PV curve for the bifurcation type that this system is subject to. Even though the MLP estimated with the traditional CPFLOW turned out to be accurate, this was not true for the total amount of DG that was disconnected. This happened because the continuation method diverged right before the nose of the PV curve, missing the units that were tripped near the critical point of the test system. The error caused by the divergence of the CPFLOW reached 27% regarding the amount of DG that is disconnected prior to MLP.

Also, from the test proposed in Fig. 5, the MLP was classified as a SIB, meaning that instability is a direct consequence of some parametric discontinuity. When the DG penetration was 10%, the static instability was due to the reactive power limit of the generator at bus 10. For the DG penetration of 20% and 30%, the trips of DG units in buses 36 and 3 were, respectively, the root causes of instability. Those disruptions resulted in cascading disconnections as can be assessed from the proposed prediction/correction and bifurcation identification schemes.

The outcome of the proposed method also comprises the sequence of discontinuities to which the power system equilibrium diagram is subject to. Between the reactive power limits and the DG mandatory disconnections, more than 200 discontinuities happen in the test system, for the three DG penetration levels considered, before the MLP is reached. Due to space limitations, only the last 5 discontinuities of the case where the DG penetration level is equal to 10% are indicated in Table III. The complete list of discontinuities that occurs during the load growth is available in [27].

The traditional CPFLOW does not provide such detailed information regarding equilibria discontinuities. At most, it can provide which discrete parametric change happened between two calculated power flow solutions. In this case, obtaining the actual sequence of DG disconnections would require very small continuation steps which would increase the computational burden. The PV curves obtained before divergence of

TABLE III: Sequence of the last 5 discontinuities of the equilibrium diagram.

Discontinuity	Bus	Voltage drop DG group	System Loading (λ)
DG	19	3	2.1115
DG	3	3	2.1108
DG	2	3	2.1108
Q-limit	113	-	2.1130
Q-limit	10	-	2.1132

the CPFLOW are shown in Fig. 7, where it is possible to see the DG discontinuities.

B. Tests Considering Undervoltage Load Shedding

Once again, the results obtained with the proposed algorithm will be compared to the ones from the CPFLOW. The following consideration were made to simplify the analysis regarding ULS:

- The undervoltage load shedding pick-up level was set equal to 0.9 pu at pre-specified load buses. When the voltage magnitude reaches this threshold, 10% of the total load (active and reactive) in the associated bus is disconnected. This setting is in accordance with what was proposed by [19].
- At the buses where ULS is possible, critical consumers that can not be turned off compose 40% of the load.
- The ULS schemes were implemented in buses 2, 3, 7, 11, 13, 14 and 117. These locations were selected based on the sensitivity analysis performed by [23].

The VSM of the system with and without the ULS can be compared in Table IV. This table also depicts the absolute amount of load that is shed and the percentage relative to the total amount (129.6 MW) that could be shed. The numerical values regarding load shedding are referred to the demand of the base case ($\lambda = 1$) and must be compared with it.

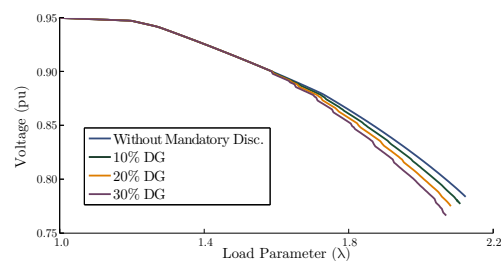


Fig. 7: Voltage Profile of bus 118 of the test system considering the DG mandatory disconnection.

This study has one essential difference when compared with the one regarding DG mandatory disconnection. This time the load discontinuities are beneficial to the voltage stability and the VSM increases for the system with ULS. For these results, both the traditional CPFLOW and the proposed algorithm converged. Notice that the biggest value of λ does not correspond to the maximum VSM anymore. This happened because the two methods employed different amounts of estimated load shed, which makes their respective relations between λ and the total power supplied distinct. Nevertheless, the value of λ_{max} indicates how further the load could be increased at

every bus without triggering the ULS scheme, which is an important information for power system operators.

TABLE IV: Effect of ULS in the test system.

Method	ULS	λ_{max}	VSM		Load shedding	
			(GW)	(%)	(MW)	(%)
CPFLOW	No	2.126	4.13	113	-	-
	Yes	2.195	4.22	115	76.2	59
Proposed	Yes	2.193	4.30	117	33.3	26

The amount of load that is shed was different for the two compared methods, as shown in the last two columns of Table IV. The CPFLOW overestimated this value due to the discrete nature of the continuation process. Two successive power flow solutions are separated by a gap that is determined by the continuation step-size employed. With the continuation method, it is not possible to isolate the events between the last stable solution and the first unstable one. Within this interval, it is not possible to determine if the load shedding occurred before or after the MLP. Since the proposed algorithm individually finds the discontinuities, it is expected to determine which discontinuities happened before the nose of the PV curve is reached, estimating the total amount of ULS more accurately.

VI. CONCLUSIONS

The proposed predictor/corrector scheme is capable to estimate the MLP of the system, classify the bifurcation type and individually identify the discontinuities in its equilibrium diagram due to DG mandatory disconnections and ULS. Furthermore, the numerical results obtained from the proposed scheme yielded important information about, for example, the mechanisms concerning cascading disconnections of DG units.

However, it is important to point out that the proposed algorithm should only be employed to manage equilibrium discontinuities produced by the events considered in this paper. In other words, its applicability is restricted to power systems that go through such discontinuities, in which case the method is expected to be more robust than the CPFLOW to determine the MLP and VSM. If that is not true, then its usage may be infeasible. This is why this procedure should not be considered to replace the traditional CPFLOW or any other standard VSA tool. On the contrary, it should be regarded as a complementary technique that could enhance the CPFLOW with new features to broaden its applicability.

A topic for a future research is to include higher order terms of the Taylor series in the discontinuity prediction step.

REFERENCES

- [1] "Ons apresenta relatório final sobre blecaute de 2009," ONS - Brazilian system operator, 2009 (in Portuguese).
- [2] V. Ajarapu, *Computational Techniques for Voltage Stability Assessment and Control (Power Electronics and Power Systems)*. Secaucus, NJ, USA: Springer-Verlag New York, Inc., 2006.
- [3] K. Yamashita, S. Djokic, J. Matevosyan, F. Resende, L. Korunovic, Z. Dong, and J. Milanovic, "Modelling and aggregation of loads in flexible power networks scope and status of the work of cigre wg c4.605," *IFAC Proceedings Volumes*, vol. 45, no. 21, pp. 405 – 410, 2012, 8th Power Plant and Power System Control Symposium.
- [4] A. Arif, Z. Wang, J. Wang, B. Mather, H. Bashualdo, and D. Zhao, "Load modeling x2013; a review," *IEEE Transactions on Smart Grid*, pp. 1–1 (Early Access), 2017.

- [5] R. A. Walling and N. W. Miller, "Distributed generation islanding-implications on power system dynamic performance," in *IEEE Power Engineering Society Summer Meeting*, vol. 1, July 2002, pp. 92–96.
- [6] P. C. Chen, V. Malbasa, and M. Kezunovic, "Analysis of voltage stability issues with distributed generation penetration in distribution networks," in *2013 North American Power Symposium (NAPS)*, Sept 2013, pp. 1–6.
- [7] H.-D. Chiang, A. J. Flueck, K. S. Shah, and N. Balu, "Cpflow: a practical tool for tracing power system steady-state stationary behavior due to load and generation variations," *IEEE Transactions on Power Systems*, vol. 10, no. 2, pp. 623–634, May 1995.
- [8] M. R. Mansour, L. F. C. Alberto, and R. A. Ramos, "Preventive control design for voltage stability considering multiple critical contingencies," *IEEE Transactions on Power Systems*, vol. 31, no. 2, pp. 1517–1525, March 2016.
- [9] C. Liu, B. Wang, F. Hu, K. Sun, and C. L. Bak, "Online voltage stability assessment for load areas based on the holomorphic embedding method," *IEEE Transactions on Power Systems*, vol. 33, no. 4, pp. 3720–3734, July 2018.
- [10] P. Xu, X. Wang, and V. Ajarapu, "Continuation power flow with adaptive stepsize control via convergence monitor," *IET Generation, Transmission Distribution*, vol. 6, no. 7, pp. 673–679, July 2012.
- [11] P. Zhu, G. Taylor, and M. Irving, "A novel q-limit guided continuation power flow method," in *2008 IEEE Power and Energy Society General Meeting - Conversion and Delivery of Electrical Energy in the 21st Century*, July 2008, pp. 1–7.
- [12] N. Yorino, H.-Q. Li, and H. Sasaki, "A predictor/corrector scheme for obtaining q-limit points for power flow studies," *IEEE Transactions on Power Systems*, vol. 20, no. 1, pp. 130–137, Feb 2005.
- [13] C. A. Canizares and F. L. Alvarado, "Point of collapse and continuation methods for large ac/dc systems," *IEEE Transactions on Power Systems*, vol. 8, no. 1, pp. 1–8, Feb 1993.
- [14] G.-Y. Cao and C. Chen, "Novel techniques for continuation method to calculate the limit-induced bifurcation of the power flow equation," *Electric Power Components and Systems*, vol. 38, no. 9, pp. 1061–1075, 2010.
- [15] I. Hiskens and B. Chakrabarti, "Direct calculation of reactive power limit points," *International Journal of Electrical Power & Energy Systems*, vol. 18, no. 2, pp. 121 – 129, 1996.
- [16] L. F. S. Colombari, M. E. C. Bento, J. A. dos Santos, and R. A. Ramos, "Procedure to account for dg mandatory disconnection during voltage stability assessment," in *2017 IEEE Manchester PowerTech*, June 2017, pp. 1–6.
- [17] R. H. Salim, R. Kuiava, R. A. Ramos, and N. G. Bretas, "Impact of power factor regulation on smallsignal stability of power distribution systems with distributed synchronous generators," *European Transactions on Electrical Power*, vol. 21, no. 7, pp. 1923–1940, 2011.
- [18] R. S. A. Abri, E. F. El-Saadany, and Y. M. Atwa, "Distributed generation placement and sizing method to improve the voltage stability margin in a distribution system," in *2nd International Conference on Electric Power and Energy Conversion Systems (EPECS)*, Nov 2011, pp. 1–7.
- [19] C. W. Taylor, "Concepts of undervoltage load shedding for voltage stability," *IEEE Transactions on Power Delivery*, vol. 7, no. 2, pp. 480–488, Apr 1992.
- [20] D. Lefebvre, C. Moors, and T. V. Cutsem, "Design of an undervoltage load shedding scheme for the hydro-quebec system," in *2003 IEEE Power Engineering Society General Meeting (IEEE Cat. No.03CH37491)*, July 2003, p. 2036 Vol. 4.
- [21] C. Moors, D. Lefebvre, and T. V. Cutsem, "Load shedding controllers against voltage instability: a comparison of designs," in *IEEE Porto Power Tech Proceedings*, 2001, p. 6 pp. vol.2.
- [22] C. M. Affonso, L. C. P. da Silva, F. G. M. Lima, and S. Soares, "Mw and mvar management on supply and demand side for meeting voltage stability margin criteria," *IEEE Transactions on Power Systems*, vol. 19, no. 3, pp. 1538–1545, Aug 2004.
- [23] T. Amraee, A. Ranjbar, B. Mozafari, and N. Sadati, "An enhanced undervoltage load-shedding scheme to provide voltage stability," *Electric Power Systems Research*, vol. 77, no. 8, pp. 1038 – 1046, 2007.
- [24] C. Moors, D. Lefebvre, and T. V. Cutsem, "Design of load shedding schemes against voltage instability," in *2000 IEEE Power Engineering Society Winter Meeting*, vol. 2, 2000, pp. 1495–1500 vol.2.
- [25] "Power systems test case archive," Institute of Electrical and Electronics Engineers (IEEE), 1996.
- [26] "One-line diagram of ieee 118-bus test system," Illinois Institute of Technology Power Group, 2003.
- [27] L. F. d. S. Colombari, "An Approach to Handle Sudden Load Changes on Static Voltage Stability Analysis," Masters Dissertation, USP, Sao Carlos, Brazil, 2017.